Article

Not peer-reviewed version

Potential of *Portulaca oleracea* Extract as a Green Reducing Agent for Silver Nanoparticle Synthesis to Enhance the Antibacterial Activity of Microcellulose Derived from Coconut Water

Eli Rohaeti *, Isti Yunita, Sri Handayani, Dini Rohmawati, Nur Aeni Ariyanti, An Nisa Kurniasari, Jin Nakamura

Posted Date: 26 February 2026

doi: 10.20944/preprints202602.1366.v1

Keywords: antimicrobial activity; glycerol; chitosan; coconut water; microcellulose; silver nanoparticles

 doi:10.20944/preprints202602.1366.v1

Article

Potential of *Portulaca oleracea* Extract as a Green Reducing Agent for Silver Nanoparticle Synthesis to Enhance the Antibacterial Activity of Microcellulose Derived from Coconut Water

Eli Rohaeti [1,*], Isti Yunita [1], Sri Handayani [1], Dini Rohmawati [1], Nur Aeni Ariyanti [2], An Nisa Kurniasari [2] and Jin Nakamura [3]

[1] Department of Chemistry Education, Faculty of Mathematics and Natural Science, Universitas Negeri Yogyakarta, Yogyakarta 55281, Indonesia
[2] Department of Biology Education, Faculty of Mathematics and Natural Science, Universitas Negeri Yogyakarta, Yogyakarta 55281, Indonesia
[3] Department of Biological Function Engeneering, Graduate School of Life Science and Systems Engineering, Kyushu Institute of Technology
* Correspondence: eli_rohaeti@uny.ac.id

Abstract

This study investigates the structural and antimicrobial properties of coconut water–derived microcellulose biocomposites incorporated with glycerol, chitosan, and silver nanoparticles. Microcellulose-based films were fabricated as silver nanoparticle–deposited microcellulose (MN), microcellulose–glycerol–silver nanoparticles (MG), microcellulose–chitosan–silver nanoparticles (MChN), and microcellulose–glycerol–chitosan–silver nanoparticles (MGChN). Antimicrobial performance was evaluated against *Pseudomonas aeruginosa*, *Staphylococcus epidermidis*, and *Candida albicans* using inhibition zone assays. The MG and MGChN films exhibited enhanced elasticity compared to MN and MChN, indicating the plasticizing effect of glycerol. Enzymatic hydrolysis using xylanase yielded microcellulose particles with sizes ranging from 1.19 to 2.07 μm and induced a bio-bleaching effect. Among all formulations, MGChN demonstrated the highest antimicrobial activity against *P. aeruginosa* and *S. epidermidis* (strong category), as well as moderate antifungal activity against *C. albicans*. Overall, the synergistic incorporation of glycerol, chitosan, and silver nanoparticles significantly improved the antimicrobial efficacy of coconut water–based microcellulose, underscoring its potential for advanced biomedical polymer applications.

Keywords: antimicrobial activity; glycerol; chitosan; coconut water; microcellulose; silver nanoparticles

1. Introduction

Indonesia, as a tropical country, possesses high biodiversity, including abundant coconut plants (*Cocos nucifera*) distributed throughout the country. Although coconuts are widely known for their extensive utilization, some parts remain underutilized, particularly coconut water. The coconut water is often discarded despite containing valuable nutrients such as potassium, sucrose, B-complex vitamins, nicotinic acid, pantothenic acid, biotin, and folic acid [1–4]. These nutrients make coconut water a promising substrate for cellulose production using *Acetobacter xylinum*. The resulting cellulose can be further converted into microcellulose through enzymatic hydrolysis using xylanase produced by bacteria such as *Bacillus* sp., *Geobacillus* sp., and *Paenibacillus* sp. [5–7]. The addition of glycerol acts as a plasticizer, improving the smoothness, flexibility, and thinness of the cellulose matrix, while chitosan and silver nanoparticles are incorporated to impart antimicrobial properties.

 doi:10.20944/preprints202602.1366.v1

Microcellulose has been extensively studied using various lignocellulosic sources, including wood, rice straw, corn cobs, pineapple leaves, bagasse, and soybean husks. Due to its non-toxic nature and excellent biocompatibility with human tissues, microcellulose has gained significant attention as a renewable biomaterial for biomedical applications, particularly as wound dressing material. However, the high prevalence of pathogenic microorganisms in the environment necessitates the incorporation of antimicrobial agents into wound coverings to prevent infection. Pathogenic bacteria and fungi can readily infect exposed tissues, especially damaged skin. According to the National Nosocomial Infection Surveillance System (NNIS), *Pseudomonas aeruginosa* is one of the most frequently isolated pathogens in wound infections [8]. In addition, *Staphylococcus epidermidis* is associated with skin infections, acne, urinary tract infections, and renal infections, while *Candida albicans* is known to cause infections of the mucosal membranes, oral cavity, vagina, and gastrointestinal tract [9–13].

Research on antimicrobial materials capable of inhibiting pathogenic bacteria and fungi is essential to support the development of effective biomedical products. Antimicrobial activity can be evaluated using several methods, including dilution-based assays that assess the formation of inhibition zones as indicators of microbial growth suppression by antimicrobial compounds [14–18]. This method involves direct exposure of test microorganisms on agar media in Petri dishes. Based on these considerations, this study focuses on the development of microcellulose biomaterials derived from coconut water, modified with glycerol and chitosan and further incorporated with silver nanoparticles, as a renewable wound dressing material with antimicrobial properties.

2. Materials and Methods

The instruments used in this study included a UV–Vis spectrophotometer (Shimadzu 1601), drying oven (CIKA PT27.221.03.058.BM), autoclave (ALP Co., Ltd., Model KT-40), incubator, digital balance (300 g capacity), magnetic stirrer–hot plate (EYELA 2000), shaker, caliper (0.0001 mm accuracy), thermometer, micropipette (100 µL), three-neck flask, Erlenmeyer flasks (1 L), beakers (500 mL), measuring cylinders (100 mL), volumetric flasks (200 mL), test tubes, Petri dishes, Drigalski spatula, Bunsen burner, pH indicator strips, and reflux apparatus. Supporting laboratory materials included plastic trays (230 × 176 × 39 mm), Mori cloth, spatulas, basins, strainers, watch glasses, aluminum foil, Whatmann No. 41 filter paper, gauze, plastic wrap, label paper, lids, latex gloves, tissues, and umbrella paper.

The materials used consisted of aged coconut water, *Acetobacter xylinum* starter, granulated sugar, urea, 70% ethanol, 3% HCl, 3% NaOH, 5% glacial acetic acid (Merck, p.a.), chitosan (2%, Merck, p.a.), pure glycerol, silver nitrate solution, trisodium citrate (10%), xylanase enzyme, purslane extract, and nutrient media including nutrient agar, sodium broth, and potato dextrose agar (PDA). Antimicrobial testing employed chloramphenicol as a positive control, *Pseudomonas aeruginosa* (FNCC 0063), *Staphylococcus epidermidis* (ATCC 35984), and *Candida albicans* (SC 5314).

2.1. Research Procedure

2.1.1. Cellulose Preparation

A total of 500 mL of filtered aged coconut water was transferred into an Erlenmeyer flask equipped with a magnetic stirrer, followed by the addition of 50 g (10%, w/v) of granulated sugar and 2.5 g (0.5%, w/v) of urea. The mixture was heated on a hot plate with continuous stirring until completely dissolved, then allowed to cool to room temperature (30 °C). Glacial acetic acid was added to adjust the pH to 4, after which the solution was aseptically dispensed into plastic trays (250 mL per tray). Subsequently, 100 mL of *Acetobacter xylinum* starter culture was inoculated into each tray, covered with parchment or sterile paper, secured with rubber bands, and incubated at room temperature for 7 days. The resulting nata de coco was harvested, washed with sterile distilled water to remove residual culture media, weighed to obtain the wet cellulose mass, and then oven-dried at 70–80 °C until a constant weight was achieved to determine the dry cellulose mass [19,20].

 doi:10.20944/preprints202602.1366.v1

2.1.2. Preparation of Cellulose-Glycerol

Filtered aged coconut water (500 mL) was placed in an Erlenmeyer flask equipped with a magnetic stirrer, followed by the addition of granulated sugar (50 g, 10% w/v), urea (2.5 g, 0.5% w/v), and glycerol (3 mL, 1.2% v/v). The mixture was heated with continuous stirring until completely dissolved, cooled to room temperature (30 °C), and adjusted to pH 4 using glacial acetic acid [21]. The solution was aseptically distributed into plastic trays (250 mL each) and inoculated with 100 mL of *Acetobacter xylinum*. The trays were covered with sterile paper, secured with rubber bands, and incubated for 7 days. The resulting nata de coco was harvested, washed with sterile distilled water, weighed to determine wet mass, and oven-dried at 70–80 °C to constant weight to obtain the dry cellulose mass.

2.1.3. Chitosan Application on Cellulose

Sheets of cellulose and cellulose bio-materials with glycerol are put into a tray containing a 2% chitosan solution and waited for chitosan to absorb. After that, the cellulose is dried in the oven at 40^0 C until the nata sheets are dry.

2.1.4. Measurement of Physical Properties of Cellulose

The wet weight of cellulose was determined by weighing the samples after 7 days of incubation. Dry weight was measured after oven-drying the cellulose at 40 °C for 7 days until a constant weight was achieved. Transparency, color, and odor were evaluated qualitatively by visual and sensory comparison among the different cellulose formulations, with odor assessment focusing on the presence of acidic smell following the 7-day incubation period.

2.1.5. Microcellulose Preparation

2.1.6. Dried Cellulose Sheets

Dried cellulose sheets (cellulose, cellulose–glycerol, cellulose–chitosan, and cellulose–glycerol–chitosan) were cut into small pieces and enzymatically hydrolyzed using a xylanase solution (1 g in 100 mL sterile distilled water) at 55 °C for 24 h. The reaction was terminated by heat treatment at 80 °C for 30 min, after which the samples were washed with distilled water and oven-dried at 45–60 °C prior to further analysis [22,23].

2.1.7. Microcellulose Size Analysis with SEM

Microcellulose samples were cut into approximately 1 × 1 cm^2 pieces and coated with a thin layer of gold prior to SEM analysis. The samples were then observed under SEM by adjusting the filament current, illumination, focus, and specimen position, and the resulting micrographs were recorded and saved for analysis.

2.1.8. Silver Nanoparticle Preparation

A 0.001 M $AgNO_3$ solution was prepared by dissolving 0.17 g of $AgNO_3$ in 1,000 mL of sterile distilled water. A 0.05% (w/v) starch solution was obtained by dissolving 0.05 g of starch in 100 mL of distilled water. Purslane extract was prepared by drying purslane leaves at 45 °C for 24 h, followed by boiling 25 g of dried leaves in 250 mL of distilled water at 80 °C for 10 min and filtering the extract using Whatman No. 41 filter paper after cooling. Silver nanoparticles were biosynthesized by mixing 10 mL of purslane extract with 65 mL of 0.001 M $AgNO_3$ solution in an Erlenmeyer flask and incubating the mixture at room temperature for 2 h, after which 25 mL of 0.05% starch solution was added as a stabilizing agent. The resulting suspension was homogenized and characterized using UV–Vis spectrophotometry and a particle size analyzer.

2.1.9. Wavelength Analysis of Silver Nanoparticles with UV Vis Spectrophotometry

 doi:10.20944/preprints202602.1366.v1

UV–Vis spectrophotometric analysis was performed by calibrating the instrument using distilled water as a blank. The absorbance spectra of the silver nanoparticle solution were recorded over a wavelength range of 200–800 nm, with characteristic surface plasmon resonance expected at 400–450 nm. The measurements were conducted by placing the sample solution in a cuvette and recording the absorbance spectrum.

2.1.10. Silver Nanoparticle Size Analysis with PSA

Particle size analysis (PSA) was performed by preheating the instrument for 20 min, after which the silver nanoparticle solution was placed into a cuvette (filled to approximately two-thirds of its volume) and analyzed according to the instrument's operating program to obtain particle size distribution data.

2.1.11. Deposition of Microcellulose in Silver Nanoparticles

Microcellulose samples with different compositional formulations were immersed in a silver nanoparticle solution and homogenized using a shaker at 145 rpm for 24 h. The resulting sheet-form materials were subsequently oven-dried and stored prior to antibacterial activity testing.

2.1.12. Antimicrobial Activity Test

Microcellulose samples with various compositions and silver nanoparticle deposition were cut into 6 mm discs and tested for antimicrobial activity using the agar diffusion method [24,25]. *Pseudomonas aeruginosa*, *Staphylococcus epidermidis*, and *Candida albicans* were cultured in nutrient broth and incubated at 30 °C for 24 h. Microbial suspensions (0.1 mL) were aseptically spread onto nutrient agar for bacteria and potato dextrose agar for fungi, after which the sample discs were placed on the inoculated media and incubated at 30 °C for 48 h. Inhibition zones were monitored at 3 h intervals for bacteria and 6 h intervals for fungi, and the inhibition zone diameters were measured using a caliper.

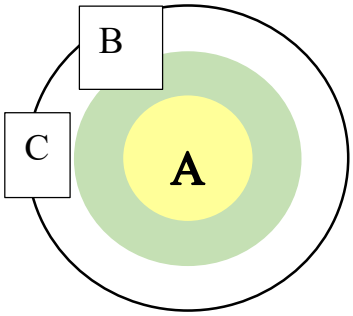

Description:
A: test sample
B: Antimicrobial zone
C: Test bacterial culture on the surface of the agar plate medium using a caliper

2.2. Data Analysis Techniques

The results obtained were tested with *one way* anova parametric statistics and further tests with DMRT (*Duncan Multiple Range Test) test.* Statistical analysis using SPSS series 20.

3. Results and Disscussion

3.1. Physical Properties of Bacterial Cellulose from Coconut Water

Cellulose sample variations were prepared by incorporating glycerol and chitosan, resulting in four formulations: cellulose without additives (C), cellulose with glycerol (CG), cellulose with chitosan (CCh), and cellulose with both glycerol and chitosan (CGCh). The prepared coconut water medium was inoculated with *Acetobacter xylinum* and fermented for 7 days to produce bacterial cellulose (nata). The physical properties of the resulting bacterial cellulose derived from coconut wastewater were evaluated in terms of wet weight, dry weight, transparency, color, consistency, and odor, and the corresponding results are presented in Table 1.

 doi:10.20944/preprints202602.1366.v1

Table 1. Physical properties of bacterial cellulose from coconut water and its variations.

Parameter	Types of Bacterial Cellulose			
	C	CG	CCh	CGCh
Wet weight	178.89 g	200.71 g	135.86 g	135.139 g
Dry weight	3.616 g	4.248 g	8.05 g	7.23 g
Transparency	Not transparent	Not transparent	Not transparent	Not transparent
Color	White	White	Brownish yellow	Brownish yellow
Consistency	Less elastic	Elastis	Less elastic	Elastis
Construction	Acidic	Acidic	Highly acidic	Highly acidic

Description: C: cellulose. CG: cellulose + glycerol. CCh: cellulose + chitosan. CGCh: cellulose + glycerol + chitosan.

Based on Table 1, variations in the wet weight of bacterial cellulose derived from coconut water were observed, with the CG formulation exhibiting the highest wet weight, followed by the C sample, indicating that glycerol addition influences cellulose formation. Cellulose is inherently hygroscopic due to the presence of hydroxyl (–OH) groups, which facilitate water absorption. Glycerol, a trihydroxy alcohol containing three hydroxyl groups, possesses strong hydrophilic and hygroscopic properties that enable it to bind water within the material matrix, thereby increasing moisture content [26,27]. In terms of consistency, the CG and CGCh samples exhibited greater elasticity than the C and CCh samples, reflecting the plasticizing effect of glycerol. Glycerol enhances the elasticity of cellulose-based biomaterials by reducing intermolecular hydrogen bonding and increasing the spacing between polymer chains, which improves polymer chain mobility and elongation capacity [28,29].

Based on the dry weight data, the CCh and CGCh formulations exhibited higher dry weights than the other samples, indicating the influence of chitosan incorporation. Chitosan contains positively charged amine ($–NH_2$) groups that can interact with negatively charged bacterial cell walls, contributing to antimicrobial activity [30,31]. In addition, chitosan coating limits water penetration into the cellulose matrix, resulting in higher dry mass after drying due to the retained chitosan content. All bacterial cellulose samples derived from coconut water were non-transparent. Noticeable color changes were observed in the CCh and CGCh samples, which can be attributed to the addition of chitosan, as chitosan dissolved in acetic acid exhibits a brownish-yellow color and imparts a pronounced acidic odor.

3.2. Microcellulose Character from Coconut Water

This section may be divided by subheadings. It should provide a concise and precise description of the experimental results, their interpretation, as well as the experimental conclusions that can be drawn.

Cellulose sample variations were treated with xylanase to induce enzymatic degradation. Xylanase is an extracellular enzyme capable of hydrolyzing polymer chains in cellulose and hemicellulose by cleaving glycosidic bonds at the terminal regions of the polymer, producing xylose and xylo-oligosaccharides as final products [32]. This hydrolytic process reduces polymer chain length, resulting in smaller particle sizes and facilitating the formation of cellulose derivatives. In this study, enzymatic hydrolysis was conducted at 55 °C using a 1% (w/v) xylanase solution for 24 h, followed by heat inactivation at 80 °C for 30 min to terminate enzyme activity. The resulting microcellulose particles exhibited lengths ranging from 50 to 180 μm. Enzymatic treatment decreased the degree of polymerization while increasing cellulose crystallinity, consistent with previous findings [33,34], and the morphology of the resulting microcellulose is shown in Figure 1.

 doi:10.20944/preprints202602.1366.v1

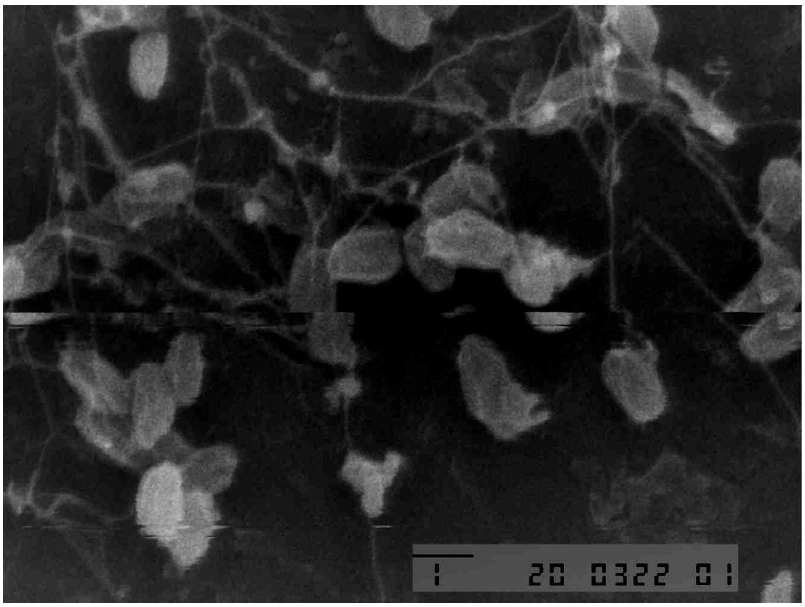

Figure 1. SEM foto of microcellulose produced from cellulose by xylanase enzyme.

In Figure 1, it can be seen that the xylanase enzyme used can degrade cellulose into microcellulose. The mycocellulosis formed has a granular shape with a particle size distribution ranging from 1.19 μm to 2.07 μm. The microcellulose that is formed has a whiter color when compared to cellulose. Based on the color observations, the resulting microcellulose exhibited a noticeably whiter appearance, which can be attributed to the bio-bleaching effect of xylanase. Xylanase facilitates the removal of non-cellulosic components from lignocellulosic materials, thereby enhancing cellulose purity and brightness. Consequently, xylanase has been widely recognized as an environmentally friendly alternative to conventional chemical bleaching processes [35,36].

3.3. Biosynthesis of Silver Nanoparticles with Purslane Extract

This section may be divided by subheadings. It should provide a concise and precise description of the experimental results, their interpretation, as well as the experimental conclusions that can be drawn.

Silver nanoparticles were synthesized from a silver nitrate ($AgNO_3$) solution using an ultrasonic method with purslane (*Portulaca oleracea*) extract as a bioreducing agent. Phytochemical compounds in purslane, particularly flavonoids and tannins containing hydroxyl (–OH) and carbonyl groups, act as electron donors that reduce Ag^+ ions into silver nanoparticles, thereby promoting stable nanoparticle formation [37].

The synthesized solution exhibited a light brown coloration that gradually intensified with increasing $AgNO_3$ concentration, indicating the reduction of Ag^+ ions and the formation of silver nanoparticles. The increase in color intensity reflects a higher concentration of nanoparticles formed in the solution. The formation of silver nanoparticles was further confirmed by UV–Visible spectrophotometry, which revealed a characteristic surface plasmon resonance (SPR) absorption band in the wavelength range of 400–500 nm, corresponding to the collective oscillation of conduction electrons on the nanoparticle surface. This SPR peak is a distinctive optical feature of silver nanoparticles and is widely used to verify their successful synthesis and optical properties [37].

The UV–Vis spectrophotometric analysis shown in Figure 2 confirms the formation of silver nanoparticles, as indicated by a characteristic absorbance peak at 430 nm with an absorbance value of 0.730, where higher absorbance reflects a greater concentration of nanoparticles. Particle size determination was subsequently carried out using a Particle Size Analyzer (PSA) based on dynamic light scattering (DLS), which measures Brownian motion resulting from collisions between particles

 doi:10.20944/preprints202602.1366.v1

and surrounding molecules; smaller particles exhibit faster motion, allowing particle diameter to be calculated from the diffusion rate during measurement.

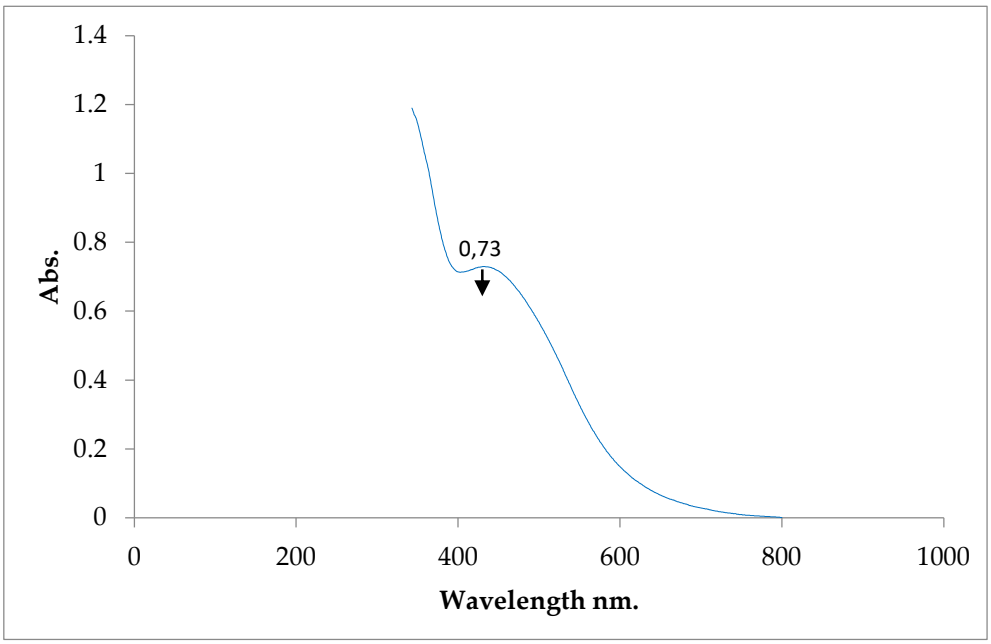

Figure 2. Results of UV Vis spectrophotometry analysis Silver Nanoparticles with Purslane Extract (*P. oleracea*).

Based on the PSA results shown in Figure 3, the synthesized silver nanoparticles exhibited an average diameter of 80.2 nm, which falls within the nanoparticle size range of 10–100 nm. Particle size measurement using PSA is considered reliable for evaluating size distribution. The size distribution of the silver nanoparticles is expressed in terms of intensity, number, and volume distributions, thereby providing a comprehensive representation of the overall particle characteristics [38,39].

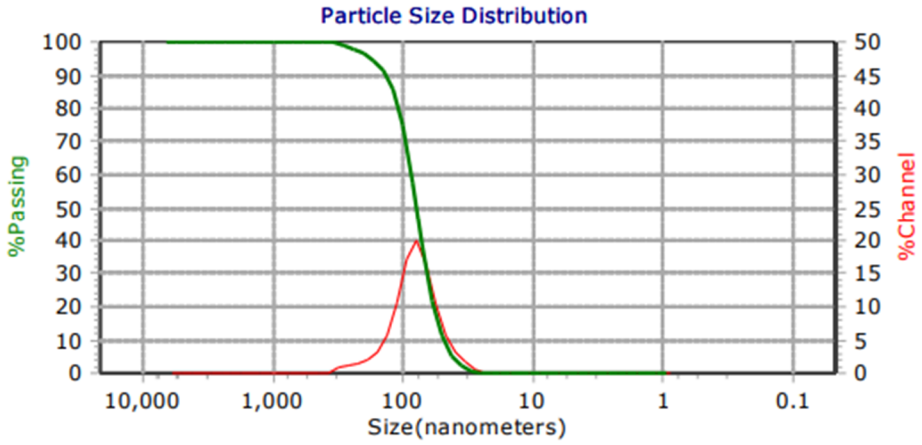

Peaks Summary		
Dia(nm)	Vol%	Width
80.2	100	61.5

Figure 3. Particle Size of Silver Nanoparticles with Purslane Extract (*P. oleracea*).

3.4. Antimicrobial Activity of Microcellulose

 doi:10.20944/preprints202602.1366.v1

Microcellulose samples treated with xylanase were immersed in previously characterized silver nanoparticles and then evaluated for antimicrobial activity against *S. epidermidis*, *P. aeruginosa*, and *C. albicans* using the Kirby–Bauer diffusion method. Inhibition zones for bacteria were measured every 3 hours and for fungi every 6 hours. The tested samples included microcellulose with silver nanoparticles (M+N), glycerol-modified microcellulose with silver nanoparticles (MG+N), chitosan-modified microcellulose with silver nanoparticles (MGCh+N). Antimicrobial activity was indicated by the formation of a clear inhibition zone around the samples and was measured in millimeters. Based on the inhibition activity is classified as weak (<5 mm), moderate (5–10 mm), strong (10–20 mm), and very strong (>20 mm) [40,41].

3.5. Antimicrobial Activity of Microcellulose Against S. epidermidis

Measurement of the inhibition zone of microcellulose sample variation against *S. epidermidis bacteria* was carried out every 3 hours for 48 hours. The results of the measurement of the inhibition zone of microcellulose sample variation against *S. epidermidis* can be seen in Figure 4.

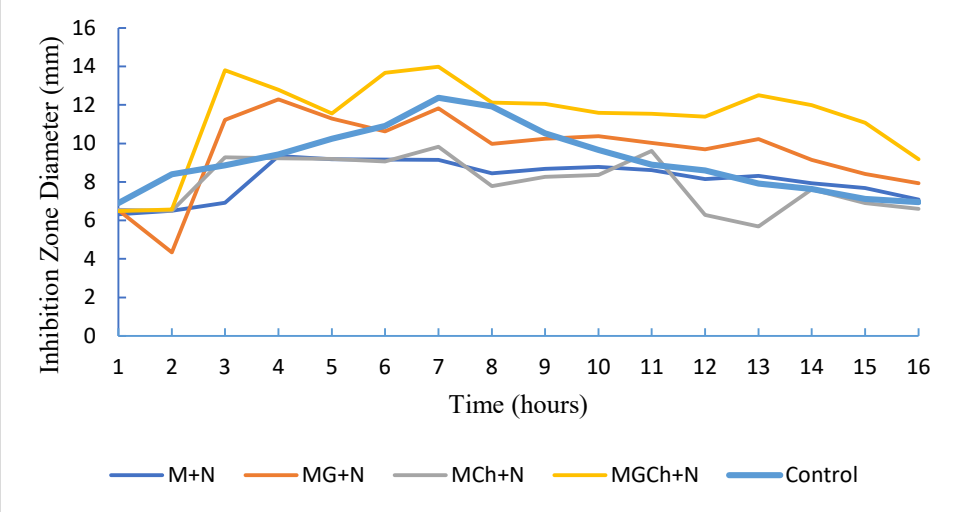

Figure 4. Antimicrobial activity of microcellulose (M+N), microcellulose-glycerol (MG+N), microcellulose-chitosan (MCh+N), and microcellulose-glycerol-chitosan (MGCh+N) against *S. epidermidis*.

Based on the graph, the MGCh+N microcellulose sample exhibited the highest inhibitory effect against *S. epidermidis*, as indicated by the formation of a clear inhibition zone surrounding the sample. However, at the 42nd hour of observation, a reduction in antimicrobial activity was observed, marked by a decrease in inhibition zone diameter due to bacterial regrowth. The reappearance of bacterial growth within the inhibition zone after prolonged incubation indicates a bacteriostatic effect. Therefore, the microcellulose variations functioned primarily as bacteriostatic agents against *S. epidermidis* [42,43].

Based on Duncan's post hoc test at a significance level of 0.05 (Table 2), three significantly different subsets were identified, indicating the presence of three groups with distinct mean inhibition zone diameters. The MGCh+N sample exhibited the largest inhibition zone and differed significantly from MCh+N, M+N, MG+N, and the control, while no significant differences were observed between MCh+N and M+N or between MG+N and the control. The highest inhibition zone diameter was recorded for MGCh+N (13.663 mm), indicating that this variation showed the strongest inhibitory effect against *S. epidermidis*. This enhanced antimicrobial activity is attributed to the combined action of chitosan and silver nanoparticles. Silver ions (Ag^+) exert antimicrobial effects by penetrating microbial cell walls and interacting electrostatically with negatively charged functional groups on cell surface proteins, such as –OH, $–NH_2$, and C=O, leading to protein inactivation [44]. In addition, Ag^+ ions form strong complexes with sulfhydryl (–SH) groups in metallothionein, resulting in S–Ag bond formation that disrupts membrane permeability and induces cellular damage [45,46].

 doi:10.20944/preprints202602.1366.v1

Silver nanoparticles can further interfere with bacterial electron transport and respiratory systems and bind to phosphate groups in DNA and RNA, thereby inhibiting replication and causing structural damage to nucleic acids.

Table 2. Further analysis of the inhibition zone *S. epidermidis* at the 21st hour with Duncan's follow-up test.

Treatment	Diameter of the inhibition zone (mm)	Category
M+N	9.1533[a]	Medium
MG+N	11.8200[b]	Strong
MCh+N	9.8400[a]	Medium
MGCh+N	13.9967[c]	Strong
Controls	12.3867[bc]	Strong

Remarks: Different notations in the same column indicate a noticeably different effect (P<0.05).

3.6. Antimicrobial Activity of Microcellulose in P. aeruginosa

Measurement of the inhibition zone of microcellulose sample variation against *P. aeruginosa* was carried out every 3 hours for 48 hours. The results of the measurement of the inhibition zone of microcellulose against *P. aeruginosa* can be seen in Figure 5.

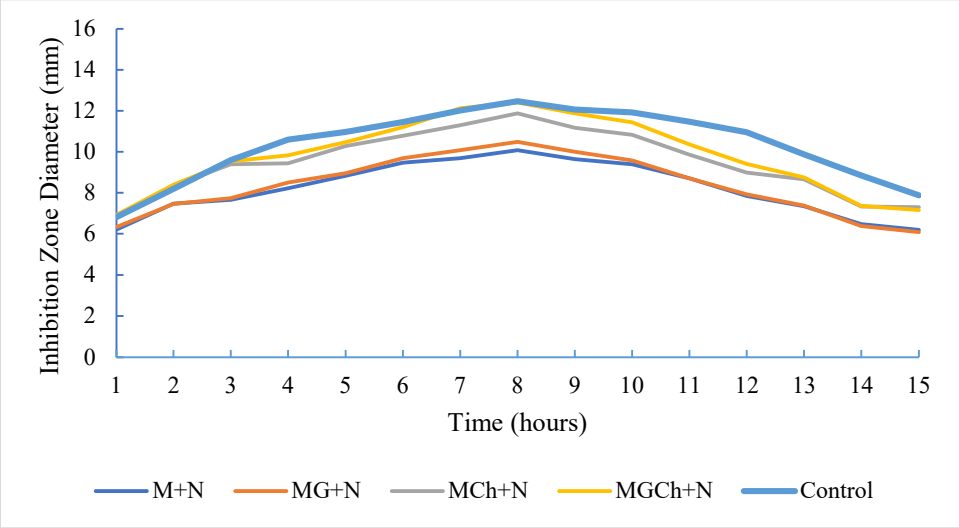

Figure 5. Antimicrobial activity of microcellulose (M+N), microcellulose-glycerol (MG+N), microcellulose-chitosan (MCh+N), and microcellulose-glycerol-chitosan (MGCh+N) against *P. aeruginosa.*

The graph indicates the formation of inhibition zones of microcellulose sample variations against *P. aeruginosa*, with MGCh+N showing the strongest inhibitory effect, as evidenced by the largest clear zone. However, a decrease in antimicrobial activity was observed at the 45th hour, marked by shrinkage of the inhibition zone due to bacterial regrowth, and at 48 hours the zone could no longer be measured because the sample was fully overgrown. Regrowth after 48 hours indicates bacteriostatic rather than bactericidal activity [42,43]. Therefore, the microcellulose sample variations function only to inhibit the growth of *P. aeruginosa*.

 doi:10.20944/preprints202602.1366.v1

Table 3. Further analysis of the inhibition zone against *P. aeruginosa* at the 24th hour with Duncan's test.

Treatment	Diameter of the barrier zone (mm)	Category
M+N	10,083[a]	Strong
MG+N	10.0497[b]	Strong
MCh+N	11,883[c]	Strong
MGCh+N	12,417[p]	Strong
Controls	12.4663[d]	Strong

Remarks: Different notations in the same column indicate a noticeably different effect (P<0.05).

Based on Duncan's post hoc test at a significance level of 0.05, four distinct subsets were identified, indicating significant differences among the M+N, MG+N, MCh+N, and MGCh+N samples. The MGCh+N sample exhibited the largest inhibition zone against *P. aeruginosa* (12.417 mm) and differed significantly from MCh+N, M+N, and MG+N, while showing no significant difference from the control. The superior antimicrobial activity of MGCh+N is attributed to the combined effects of chitosan and silver nanoparticles; although chitosan exhibits antibacterial properties, its activity decreases when immobilized in membrane form, necessitating reinforcement by silver nanoparticles [47,48]. Silver ions exert antimicrobial action by penetrating bacterial cell walls, binding to sulfhydryl groups, inhibiting enzyme activity and DNA synthesis, ultimately leading to cell death. The smaller inhibition zones observed against *P. aeruginosa* compared to *S. epidermidis* are associated with fundamental differences in cell wall structure: Gram-negative bacteria possess an outer lipopolysaccharide membrane that limits nanoparticle penetration, whereas Gram-positive bacteria have a thicker peptidoglycan layer that differently influences AgNPs interaction and binding, affecting antimicrobial susceptibility [49–51].

3.7. Antimicrobial Activity of Microcellulose Against C. albicans

Measurement of the inhibition zone of microcellulose sample variation against *C. albicans fungi* was carried out every 6 hours for 48 hours. The results of the measurement of the inhibition zone of microcellulose sample variation against *the fungus C. albicans* can be seen in Figure 6.

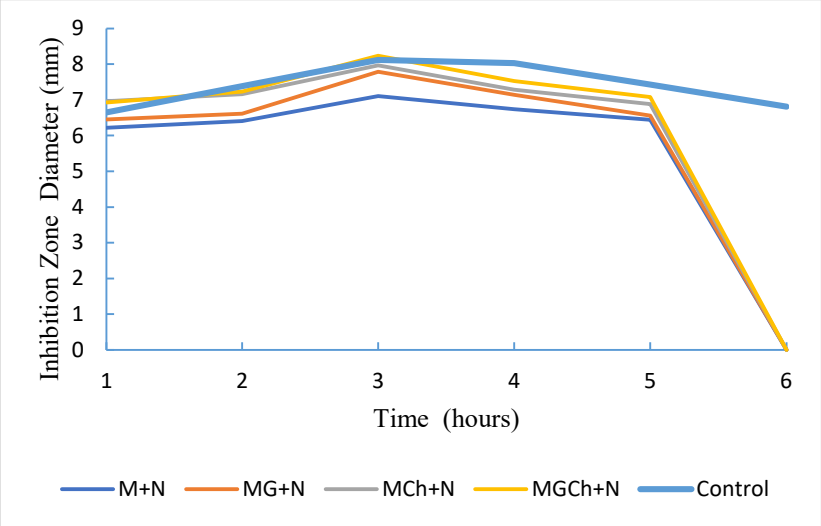

Figure 6. Antimicrobial activity of microcellulose (M+N), microcellulose-glycerol (MG+N), microcellulose-chitosan (MCh+N), and microcellulose-glycerol-chitosan (MGCh+N) against *C. albicans.*

 doi:10.20944/preprints202602.1366.v1

The inhibition zone profiles of the microcellulose sample variations against *Candida albicans* revealed that the MGCh+N formulation exhibited the highest antifungal activity. However, a progressive decline in antifungal efficacy was observed after 30 h of incubation, as evidenced by a reduction in the diameter of the clear inhibition zone due to fungal regrowth. By 36 h, no discernible inhibition zone was detected. These findings indicate that all silver nanoparticle-deposited microcellulose formulations exerted a fungistatic rather than fungicidal effect, effectively suppressing the growth of *C. albicans* for up to 36 h without complete eradication.

Table 4. Further analysis of *the inhibition zone of C. albicans* at the 18th hour with Duncan's follow-up test.

Treatment	Diameter of the inhibition zone (mm)	Category
M+N	7.1100[a]	Medium
MG+N	7.7933[a]	Medium
MCh+N	7.9733[b]	Medium
MGCh+N	8.1200[b]	Medium
Controls	8.2433[b]	Medium

Remarks: Different notations in the same column indicate a noticeably different effect (P<0.05).

Based on Duncan's post hoc test at a significance level of 0.05, two distinct subsets were identified. The M+N and MG+N samples did not differ significantly, while MCh+N, MGCh+N, and the control formed another subset and differed significantly from M+N and MG+N. The MGCh+N sample exhibited the largest inhibition zone (8.2433 mm). Antifungal efficacy against *Candida albicans* is modulated by the structural complexity of the fungal cell wall and membrane composition, which can limit nanoparticle penetration and ROS-mediated damage. Silver nanoparticles exert antifungal effects by disrupting cell membrane integrity, increasing cellular permeability, and inducing oxidative stress, with effectiveness influenced by nanoparticle concentration and fungal physiology [52–54].

4. Conclusions

Xylanase can produce microcellulose with particle sizes of 1.19–2.07 μm and induce a bio-bleaching effect. Microcellulose synthesized with glycerol–silver nanoparticles (MGN) and glycerol–chitosan–silver nanoparticles (MGChN) exhibited higher elasticity than microcellulose–silver nanoparticles (MN) and microcellulose–chitosan–silver nanoparticles (MChN). Microcellulose derived from coconut water with the addition of glycerol and chitosan and deposited with silver nanoparticles showed inhibitory activity against *P. aeruginosa* FNCC 0063, *S. epidermidis* ATCC 35984, and *C. albicans* SC 5314. The MGCh+N variation demonstrated the strongest antibacterial activity against *P. aeruginosa* and *S. epidermidis*, while exhibiting moderate antifungal activity against *C. albicans*.

Author Contributions: E.R. proposed the concept, wrote the manuscript, participated in data analysis and manuscript discussion, and also supervision. N.A.A. and A.N.K. performed the experiments. I.Y. participated in data analysis, manuscript discussion, and the preparation of publication manuscript. D.R. conducted the characterization. S.H. proposed the concept, participated in data analysis and manuscript discussion. J.N. participated in data analysis and manuscript discussion, and also supervision. All authors have read and agreed to the published version of the manuscript.

Funding: This research was funded by EQUITY PTNBH UNY YEAR 2025 via scheme Research on Strengthening the Reputation of the Scientific Field (Riset Penguatan Reputasi Bidang Keilmuan) with no. Contract 15/DST/UN34.9/T/PT.01.03/2026.

Institutional Review Board Statement: Not applicable.

 doi:10.20944/preprints202602.1366.v1

Data Availability Statement: All relevant data are included in the article.

Acknowledgments: The authors would like to thank EQUITY PTNBH UNY YEAR 2025 for the Research on Strengthening the Reputation of the Scientific Field (Contract No. 15/DST/UN34.9/T/PT.01.03/2026) and LPDP by RIIM 4 for financial support (Contract No. 150/IV/KS/11/2023 and T/42/UN34.9/PT.01.03/2023). The authors also acknowledge all collaborators for their contributions to data analysis, characterization, and manuscript preparation.

Conflicts of Interest: The authors declare no conflicts of interest.

References

1. Shi, S.; Wang, W.; Wang, F.; Yang, P., Yang, H., He, X., & Liao, X. Research Progress in Coconut Water: A Review of Nutritional Composition, Biological Activities, and Novel Processing Technologies. *Foods* **2025,** *14,* 1503.
2. Zhang, Y.; Kan, J.; Liu, X.; Song, F.; Zhu, K.; Li, N.; & Zhang, Y. Chemical Components, Nutritional Value, Volatile Organic Compounds and Biological Activities In Vitro of Coconut (Cocos nucifera L.) Water with Different Maturities. *Foods* **2024,** *13,* 863.
3. Aba, R. P. M.; Luna, M. B. Z.; & Villasis, J. C. Characterization of mature coconut (Cocos nucifera L.) water from different varieties. *Food Humanit.* **2024,** 100248.
4. Selvaraju, V. P.; Gayathri, Ranpatabendi, T.; & Fiore, A. Matured coconut water–nutritional profile and preservation methods. *Coconut-Based Beverages Prod.* **2025,** 55–78 doi:https://doi.org/10.1016/B978-0-443-26532-7.00006-X.
5. Menshawy, M. N.; Abdel-Hamid, A. M.; & El-Katatny, M. H. Maximizing cellulase and xylanase production from Novel Bacillus pumilus strain isolated from agricultural waste compost in Egypt and optimizing their activities. *Discov. Appl. Sci.* **2025,** *7*.
6. Rivas-Zúñiga, A.; Eceiza, A.; & Fernández-d'Arlas, B. A mechano-enzymatic method to produce nano/microcellulose with ancestral endoglucanase: A comparative study. *Nanoscale Adv.* **2025,** *7,* 5625–5636.
7. Chen, M.; Li, Q.; Liu, C.; Meng, E.; & Zhang, B. Microbial Degradation of Lignocellulose for Sustainable Biomass Utilization and Future Research Perspectives. *Sustainability* **2025,** *17,* 1–22.
8. Esfahani, S. N. M.; Rostami, S.; & Amini, Z. Antibiotic Susceptibility Pattern of Nosocomial and Community-Acquired Pseudomonas aeruginosa in Isfahan : Prospective Multicenter Study. *Kermanshah Univ Med Sci.* **2024,** *28,* 1–7.
9. Jurševics, K.; Rudenko, L.; Vetra, J.; & Berzins, A. Adhesion and Colonization Intensity of Staphylococcus epidermidis , Pseudomonas aeruginosa , and Candida albicans on Smooth , Micro-Textured , and Macro-Textured Silicone Biomaterials. *J. Funct. Biomater.* **2025,** *16,* 1–12.
10. Scalia, A. C. & Najmi, Z. Targeting Bacterial Biofilms on Medical Implants : Current and Emerging Approaches. *antibiotics* **2025,** *14,* 1–33.
11. Valentine, M.; Wilson, D.; Gresnigt, M. S.; & Hube, B. Vaginal Candida albicans infections : host – pa thogen – microbiome inter actions. *FEMS Microbiol. Rev.* **2025,** *49,* 1–16.
12. An, C.; Liu, Y.; Zhang, X.; Li, J.; & Chen, H. Iron dictates the growth , biofilm formation , and virulence of Pseudomonas aeruginosa in pulmonary infections. *Front. Microbiol.* **2026,** *16,* 1–12.
13. Hurley, J. Associations Between Candida and Staphylococcus aureus , Pseudomonas aeruginosa , and Acinetobacter Species as Ventilator-Associated Pneumonia Isolates in 84 Cohorts of ICU Patients. *microorganisms* **2025,** *13,* 1–18.
14. Gonzalez-pastor, R.; Carrera-Pacheco, S. E.; Zuniga-Miranda, J.; Rodriguez-Polit, C.; Mayorga-Ramos, A.; Guaman, L. P.; & Barba-Ostria, C. Current Landscape of Methods to Evaluate Antimicrobial Activity of Natural Extracts. *Molecules* **2023,** *28,* 1–25.
15. Hulankova, R. Methods for Determination of Antimicrobial Activity of Essential Oils In Vitro—A Review. *Plants* **2024,** *13,* 1–23.
16. Benkova, M.; Soukup, O.; & Marek, J. Antimicrobial susceptibility testing : currently used methods and devices and the near future in clinical practice. *J. Appl. Microbiol.* **2020,** *129,* 806--822.

 doi:10.20944/preprints202602.1366.v1

17. Kadeřábková, N.; Mahmood, A. J. S.; & Mavridou, D. A. I. Antibiotic susceptibility testing using minimum inhibitory concentration (MIC) assays. *Antimicrob. Resist.* **2024,** *2,* 1–9.
18. Krapienis, M. G. & Lourenço, F. R. Agar diffusion microbiological assays for antibiotic potency estimation: Improvements in measurement and uncertainty analysis. *J. Microbiol. Methods* **2024,** *216*.
19. Fei, S.; Fu, M.; Kang, J.; Luo, J.; Wang, Y.; Jia, J.; Liu, S.; & Li, C. Enhancing bacterial cellulose production of Komagataeibacter nataicola through fermented coconut water by Saccharomyces cerevisiae : A metabonomics approach. *Curr. Reserach Food Sci.* **2024**, *8,* 1–9.
20. Phan, H. T.; Hoang, D. Q.; Nguyen, T.; & Le, D. H. Nata de coco as an abundant bacterial cellulose resource to prepare aerogels for the removal of organic dyes in water. *Bioresour. Technol. Reports* **2023,** *24*.
21. Liu, Q.; Zhang, H.; Chen, Y.; & Wang, J. Combined biosynthetic modulation and network fortification to improve nata de coco production. in *Materials Today: Proceedings* **2025,** 123–134.
22. Matos, J. M. S.; Evtuguin, D. V.; de Sousa, A. P. M. & Carvalho, M. G. V. S. Xylanase treatment of eucalypt kraft pulps : effect of carryover. *Appl. Microbiol. Biotechnol.* **2024,** *108,* 1–13.
23. Morán-Aguilar, M. G.; Calderón-Santoyo, M.; de Souza Oliveira, R. P.; Aguilar-Uscanga, M. G.; & Domínguez, J. M. Enzyme mixtures rich in cellulase and xylanase applied to cellulose pulps for modification and hydrolysis. *Materials (Basel).* **2024,** *18,* 4968.
24. Munir. Production, characterization, and antimicrobial activity of polyhydroxyalkanoates synthesized by Bacillus species against skin pathogens. *RSC Adv.* **2025,** *15*, 35182–35200.
25. Skowron, K.; Budzyńska, A.; Wiktorczyk-Kapischke, N.; Warzonkoska, W.; Gospodarek-Komkowska, E.; & Grudlewska-Buda; K. Assessment of antimicrobial efficacy in selected antibacterial cosmetics *. *Pomeranian J Life Sci*. **2024,** *70*, 74–82.
26. Akachat, B. Effect of glycerol concentration on the physicochemical properties of pectin films derived from Citrus limon waste. *Foods* **2025,** *14,* 1576.
27. Karnwal, A. Advanced starch-based films for food packaging : Innovations in sustainability and functional properties. *Food Chem. X* **2025,** *29*, 1–21.
28. Li, J.; Chen, Z.; & Zhu, H. Effect of glycerol plasticizer on the physical and mechanical properties of cellulose films extracted from plant fibres. *Polymers (Basel).* **2023,** *15*, 2458.
29. Smith, A. R. & Gupta, B. Influence of glycerol plasticization on the structural, mechanical, and thermal properties of cellulose-based composites. *J. Appl. Polym. Sci.* **2025,** *142*, e54567.
30. Darmenbayeva, A.; Zhussipnazarova, G.; Rajasekharan, R.; Massalimova, B.; Zharlykapova, R.; Nurlybayeva, A.; Mukazhanova, Z.; Aubakirova, G.; Begenova, B.; Manapova, S.; & Bulekbayeva, K. Applications and Advantages of Cellulose – Chitosan Biocomposites : Sustainable Alternatives for Reducing Plastic Dependency. *Polymers (Basel).* **2025,** *17*, 1–15.
31. Wang, H.; Zhang, Z.; Wang, S.; Chai, X.; Li, K.; & Feng, J. Bioinspired chitosan coatings enhanced with bacterial cellulose nanocrystals and apple polyphenols for preservation of perishable fruits. *Food Chem.* **2025,** *410*.
32. Carvalho, L. da S. C. de.; Brenes, R. G. R.; Grieco, M. A.; Bojorge, N.; Jr, N. B. Production of cellulose nano/microfibers through simultaneous milling and enzymatic hydrolysis with an optimized cocktail of cellulase/xylanase/LPMO. *Ind. Crops Prod.* **2024,** *220.*
33. Benini, K. C. C. de C.; Yupanqui-Mendoza, S. L.; & Arantes, V. Impact of enzymatic hydrolysis and drying on cellulose nanocrystal properties. *Carbohydr. Res.* **2025,** *555.*
34. Rivas-Zuñiga, A.; Eceiza, A.; & Fernandez-d'Arlas, B. A mechano-enzymatic method to produce nano / microcellulose with ancestral. *Nanoscale Adv.* **2025,** *7*, 5625–5636.
35. Guo, W.; Hui, L.; Song, F.; Qu, Y.; Wang, Q.; Zhang, Y.; & Xin, J. A new strategy for biological enzyme bleaching: combined effects of laccase, xylanase, and mannanase in the bleaching of softwood kraft pulp – a synergistic effect of enzymes. *Nord. Pulp Pap. Res. J.* **2025,** *40,* 465–476.
36. Andrades, D. De, Sandrim, V. C.; Andrades, D. De; & Sandrim, V. C. Agro-residue Valorization for Thermostable Xylanase Production by Aspergillus caespitosus and its Eco- friendly Application in Pulp Biobleaching Agro-residue Valorization for Thermostable Xylanase Production by Aspergillus caespitosus and its Eco- friendl. *BioResources* **2026,** *21*, 1690–1705.

 doi:10.20944/preprints202602.1366.v1

37. Abdel-rahman, M. A.; Alshallash, K. S.; Eid, A. M.; Hassan, S. E.; Salih, M.; Hamza, M. F.; & Fouda, A. Exploring the Antimicrobial , Antioxidant , and Antiviral Potential of Eco-Friendly Synthesized Silver Nanoparticles Using Leaf Aqueous Extract of Portulaca oleracea L . *Pharm. Artic.* **2024,** *17*, 1–19.
38. Rodriguez-loya, J.; Lerma, M.; & Gardea-torresdey, J. L. Dynamic Light Scattering and Its Application to Control Nanoparticle Aggregation in Colloidal Systems : A Review. *micromachines Rev.* **2024,** *15*, 1–21.
39. Jia, Z.; Li, J.; Gao, L.; Yang, D.; & Kanaev, A. Dynamic Light Scattering : A Powerful Tool for In Situ Nanoparticle Sizing. *colloids and interfaces* **2023,** *7*, 1–18.
40. Iwani, M.; Wibowo, R. H.; & Handayani, K. Classification of antibacterial activity based on inhibition zone diameter in agar diffusion assays. *Adv. Healthc. Res.* **2025,** *3*, 510–518.
41. Wardani, N. P.; Primaharinastiti, R.; Poernomo, A. T.; & Khatib, A. A comparative study of honey antimicrobial activity against MRSA and Candida albicans based on inhibition zone diameters. *J. Farm. dan Ilmu Kefarmasian Indones.* **2024**, *12*, 89–97.
42. Karlo, J.; Vijay, A.; Phaneeswar, M. S.; & Singh, S. P. Sensing the Bactericidal and Bacteriostatic Antimicrobial Mode of Action Using Raman Deuterium Stable Isotope Probing (DSIP) in Escherichia coli. *ACS Omega* **2024,** *9*, 23753–23760.
43. Liang, Y.; Heining, L.; Elsner, M.; & Seidel, M. Flow cytometry for rapid analysis of bacteriostatic versus bactericidal effects in Legionella pneumophila disinfection. *Anal. Bioanal. Chem* **2025**. doi:10.1007/s00216-025-06055-z.
44. Dube, E. & Okuthe, G. E. Silver Nanoparticle-Based Antimicrobial Coatings : Sustainable Strategies for Microbial Contamination Control. *Microbiol. Res. (Pavia).* **2025,** *16*, 1–38.
45. Soleimani, S. Exploiting silver ions ' antimicrobial properties for colorimetric detection of Salmonella via suppressed formation of Au @ Ag nanorods. *Sci. Rep.* **2025,** *15*, 1–13.
46. Casals, E.; Gusta, M. F.; Bastus, N.; Rello, J.; & Puntes, V. Silver Nanoparticles and Antibiotics : A Promising Synergistic Approach to Multidrug-Resistant Infections. *microorganisms* **2025**, *13*, 1–18.
47. Behera, S. S.; Majumdar, A. G.; Gullani, H.; Roy, A. L.; Dash, A. K.; Mohanty, P.S.; & Ray, L. Green synthesis of silver-chitosan nanocomposite exhibits promising antibiofilm properties against pathogenic bacteria Escherichia coli and Staphylococcus aureus. *The Micobe* **2025,** *6*, 1–10.
48. Pastrana-alta, R. Y.; Huarote-garcia, E.; Egusquiza-Huamani, M. A.; & Baena-Moncada, A. M. Antimicrobial activity of chitosan, alginate, pectin, and cellulose-based biopolymer composites with silver, copper oxide, and zinc oxide nanoparticles. *RSC Adv.* **2025,** *15*, 35807–35843.
49. Frippiat, T.; Art, T.; & Delguste, C. Silver Nanoparticles as Antimicrobial Agents in Veterinary Medicine : Current Applications and Future Perspectives. *Nanomaterials* **2025**, *15*, 1–28.
50. Dybkova, S. Antimicrobial efficiency of 'green' silver nanoparticles: Influence of bacterial cell wall structure. *Materials (Basel).* **2025,** *18*, 4952.
51. Rodrigues, A. S.; Batista , J. G. S.; Rodrigues, M. A. V.; Thipe, V. C.; Minarini, L. A. R.; Lopes, P. S.; & Lugão, A. B. Advances in silver nanoparticles : a comprehensive review on their potential as antimicrobial agents and their mechanisms of action elucidated by proteomics. *Front. Microbiol.* **2024,** *15*.
52. Gao, Y.; Cao, Q., Xiao, Q., Wu, Y.; Ding, L.; Huang, H.; Li, Y.; Yang, J.; & Meng, L. The progress and future of the treatment of Candida albicans infections based on nanotechnology. *J. Nanobiotechnology* **2024,** *22*, 1–23.
53. Chandrakar, N.; Shukla, S. K.; Karley, D.; Upadhyay, N.; & Nancharaiah, Y. V. Biogenic Silver Nanoparticles Exhibit Antifungal and Antibiofilm Activity Against Candida albicans via Intracellular ROS Production. *J. Pathol. Microbiol. Immunol.* **2025,** *133*, 1–9.
54. Almotairy, A. R. Z. Novel synthesis and potential antifungal activity of silver nanospheres and nanotriangles against Candida spp. *J. Appl. Microbiol.* **2024**, *127*, 198–209.